1 Transport of carboxylate salts of varying chain lengths in

crosslinked polyether membranes

2

9

Antara Mazumder¹, Alexandra Heist², Bryan S. Beckingham^{1,*}

¹Department of Chemical Engineering, Auburn University, Auburn, AL 36849, United States

²Department of Mechanical Engineering, Washington University, St. Louis, Missouri, United

States

*Corresponding Author: Tel: +1 (334) 844-2036

E-mail Address: bsb0025@auburn.edu (Bryan S. Beckingham)

Abstract.

10

11

12

13

14

15

16

17

18

19

20

21

22

23

24

25

26

27

28

29

30

31

32

Carboxylate anions of various chain lengths are important molecules for many applications such as CO₂ reduction, membrane-based bioreactors, etc. Also, carboxylate anions are ubiquitous in biological molecules such as amino acids, fatty acids, etc. Therefore, understanding the transport behavior of carboxylates of different chain lengths in polymer materials is important both as a fundamental phenomenon but also for designing materials for applications. Here, we characterized transport behavior by measuring the permeability (P), and total partition coefficient (K) for a series of polymer membranes for four model carboxylate salts—sodium salts of formate (NaOFm), acetate (NaOAc), propionate (NaOPr), and butanoate (NaOBu)—at varied upstream salt concentrations (0.1 to 1M) or a series of polyethylene glycol diacrylate (PEGDA)-based membranes with 1) varying pre-polymerization water content; 2) varying uncharged side chain comonomer (polyethylene glycol methacrylate, PEGMA), and 3) varying charged comonomer)2acrylamido-2-methyl-1-propanesulfonic acid, AMPS). Also, diffusivity values of the four salts through the membranes have been calculated based on the solution diffusion model equation $(P=K\times D)$, experimentally obtained permeability, and total partition coefficients. For a majority of these membranes, NaOFm's permeability is much higher than the other three carboxylate salts (NaOAc, NaOPr, and NaOBu) seemingly due to the lower chain length and thereby smaller hydrated diameter. In terms of total partition coefficient, a size-based trend is not observed. For example, NaOBu's total partition coefficient (K) is generally the largest among the four, and at higher upstream salt concentrations (1M), the values of the total partition coefficients of the four salts converge. From this we conclude that the carboxylate salt transport through these PEGDAbased non-porous dense membranes to be primarily driven by kinetics and not sorption.

Keywords. Permeability; Carboxylate Salts; PEGDA; AMPS; PEGMA

Introduction

33

34

35

36

37

38

39

40

41

42

43

44

45

46

47

48

49

50

51

52

53

54

55

Electrochemical cells are an attractive approach for CO₂ utilization ¹⁻³ for the production of valuable chemicals/fuels while reducing anthropogenic CO₂ ⁴⁻⁸. A typical electrochemical cell consists of a cathode (e.g., copper foil) where the CO₂ reduction process occurs and an anode (e.g., platinum foil) where an oxygen evolution reaction takes place where both electrodes interface with an electrolytic solution (e.g., NaHCO₃)^{8,9}. These electrochemical half-cells are separated by an ion exchange membrane (IEM), a significant element of an electrochemical cell. The vital role of IEMs here is to allow the pertinent ion transport for operating the electrochemical reduction process and limiting the crossover of products which reduces the electrochemical cell efficiency^{8–} ¹⁰. An electrochemical reaction generally occurs at the electrode-electrolyte interface and involves four elementary steps. They are (1) the chemical adsorption of CO₂ molecules, (2) the chemical activation of CO₂ to the intermediate radical CO₂•-, (3) the multiple electron/proton transfer process to form carbonaceous products, and (4) the desorption of products from electro-catalyst surface^{6,11,12}. Due to multiple electron-proton pathways, a series of products are typically produced in the cathode chamber based on the electro-catalyst type and operating conditions ^{6,11}. These products can include carbon monoxide (CO), formic acid (HCOOH), methanol (CH₃OH), formaldehyde (HCHO), methane (CH₄), ethylene (C₂H₄), formate (HCOO⁻), acetate (CH₃COO⁻), etc. A study by Kuhl et al. (2012) showed that, although an anion exchange membrane was used to separate the working and counter electrode compartments to prevent the oxidation of reduced CO₂ products, it couldn't preclude passage of the CO₂ reduction products acetate and formate from the cathodic to anodic chamber¹³. Therefore, the limited capability to prevent reduction products crossover across the IEMs compels the improvement in the design parameters of membranes for electrochemical cell applications. More broadly, ion exchange membranes (IEMs) are fundamental

components utilized in other energy and separation applications, such as in water purification¹⁴, redox flow battery cells¹⁵, electrodialysis (ED)^{16,17}, etc. Therefore, it is important to study and understand membrane structure-property relationships for improving the design of ion exchange membranes (IEMs) overall.

56

57

58

59

60

61

62

63

64

65

66

67

68

69

70

71

72

73

74

75

76

77

There has been considerable study of the transport of inorganic salts such as NaCl, KCl, and MgCl₂ through ion-exchange membranes with varied morphological and chemical properties ^{18–22}. For instance, a study by Yan et al. (2018) investigated the transport of NaCl through cation exchange membranes (CEM), fabricated using PEGDA poly(ethylene glycol) diacrylate (PEGDA) and AMPS (2-acrylamido-2-methylpropane sulfonic acid)¹⁸. In another study by Geise et al. (2014), membrane potential and permselectivity were measured for four commercially available ion exchange membranes (both cation and anion exchange membranes) using aqueous solutions of sodium chloride (NaCl), ammonium chloride (NH₄Cl), sodium bicarbonate (NaHCO₃), and ammonium bicarbonate (NH₄CO₃)²². From this study, it was hypothesized that counter-ion binding affinity with polymer fixed charge groups and co-ion charge density might play an essential role in determining membrane permselectivity. However, of interest to us for electrochemical CO₂ reduction are formate (HCOO⁻) and acetate (CH₃COO⁻), which are two of the sixteen reported CO₂ reduction products produced using copper (Cu) cathodes¹³. There have been considerably fewer studies of the transport of carboxylate salts such as these transport through structurally varied IEMs. Previously, in a series of studies we investigated the transport and cotransport behavior of sodium formate, and sodium acetate with alcohols (methanol and ethanol) through different membrane chemistries towards better understanding the CO₂ reduction product crossover problem and associated membrane structure-property relationships^{23–29}.

Some significant factors for water or salt transport through polymer membranes are hydration number, salt dissociation factor, and the coulombic interaction between the counter-ion and the ionic group. Carboxylate salts/anions possess both hydrophilic and hydrophobic components that are associated with both hydrophobic and hydrophilic hydration³⁰. For instance, the primary difference between formate and acetate is the length of the hydrophobic chain. Hydrophobic hydration arises from hydrocarbon constituents of the molecular structure, and at the same time, hydrophilic (nucleophilic and electrophilic) interactions with water are dominated by electron donor/acceptor atoms and the negative charge group (RCOO⁻) present ^{30–32}. Also, the interaction between the carboxylate anions and cations is quite exciting and another critical aspect to consider³⁰. Previously, hydration studies of carboxylate transport have been performed by infrared spectroscopy, vibrational spectroscopy, or diffractive studies ^{30,32,33}. Also, carboxylate anions in aqueous solutions have been studied with various computational approaches, such as classical and quantum molecular dynamic simulations ^{32,34}. Based on those works, we conjectured that carboxylate anions having both hydrophobic and hydrophilic structures may impact the mobility of the sodium ions (Na⁺) through different membrane structures in disparate ways and prompted us to investigate the transport behavior of carboxylate salts of various chain lengths through distinct membrane chemistry. Since carboxylate groups are omnipresent in biological molecules, mostly in amino acids, fatty acids, lipid bilayers, etc., this study could also be a helpful investigation for understanding transport-related phenomena in biological systems/applications. Solute transport through the dense/non-porous membranes is defined by the solution-diffusion model or sorption/migration mechanism ^{35–37}. In this mechanism, at first, the solute sorb in the membrane interface thus partitions into the membrane (parallel to the "solution") and subsequently migrates across the membrane under a potential gradient (concentration). For the ion exchange

78

79

80

81

82

83

84

85

86

87

88

89

90

91

92

93

94

95

96

97

98

99

membranes (IEMs), the ion sorption in the membrane matrix is governed by the thermodynamic equilibrium of the electrochemical potential between the bulk solution and membrane matrix, which is defined by the electrostatic potential difference across the solution-membrane interface, termed as Donnan potential. Generally, the IEMs with high charge absorb a significantly greater number of counterions (ions with opposite direction to that of a fixed charge) than co-ions (ions similar to the fixed charge) to balance the fixed charge groups electrically. Thus, we are interested in how charge-neutral and charged membranes interact with different carboxylate salts at various upstream concentrations. In this study, we investigate the transport behavior for four carboxylate salts—sodium formate (NaOFm), sodium acetate (NaOAc), sodium propionate (NaOPr), and sodium butanoate (NaOBu) (see Figure 1 for structures)—through PEGDA-based membranes at three upstream solution concentrations (0.1, 0.5, and 1M). The membrane synthesis consists of PEGDA as the crosslinker, monoacrylate comonomers as structure modifiers, AMPS as a monoacrylate charged monomer, and prepolymerization water content which acts as the solvent and whose content can be varied to impact the membrane fractional free volume²⁸. We thereby synthesize membranes of varied fractional free volume in three different ways: 1) varying pre-polymerization water content (wt.%), 2) varying side chain comonomer content [here PEGMA poly(ethylene glycol) methacrylate (PEGMA, n=9)], and 3) varying fixed charge group AMPS content following the scheme showed in Figure 2. Synthesized films are characterized for their permeabilities (P, cm²s⁻¹) and total ion partition coefficient (K, dimensionless) to the four carboxylate salts by diffusion cell experiments and sorption-desorption experiments respectively.

101

102

103

104

105

106

107

108

109

110

111

112

113

114

115

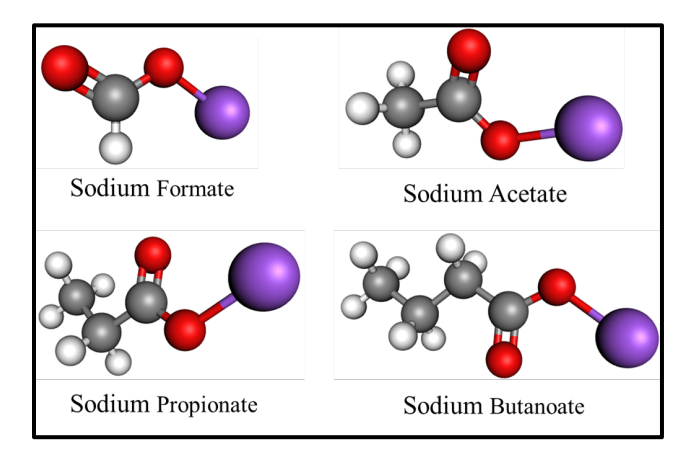
116

117

118

119

120



- Figure 1: Chemical Structures of target carboxylate salts. (A) Sodium Formate (NaOFm) (B)
- Sodium Acetate (NaOAc) (C) Sodium Propionate (NaOPr) (D) Sodium Butanoate (NaOBu).

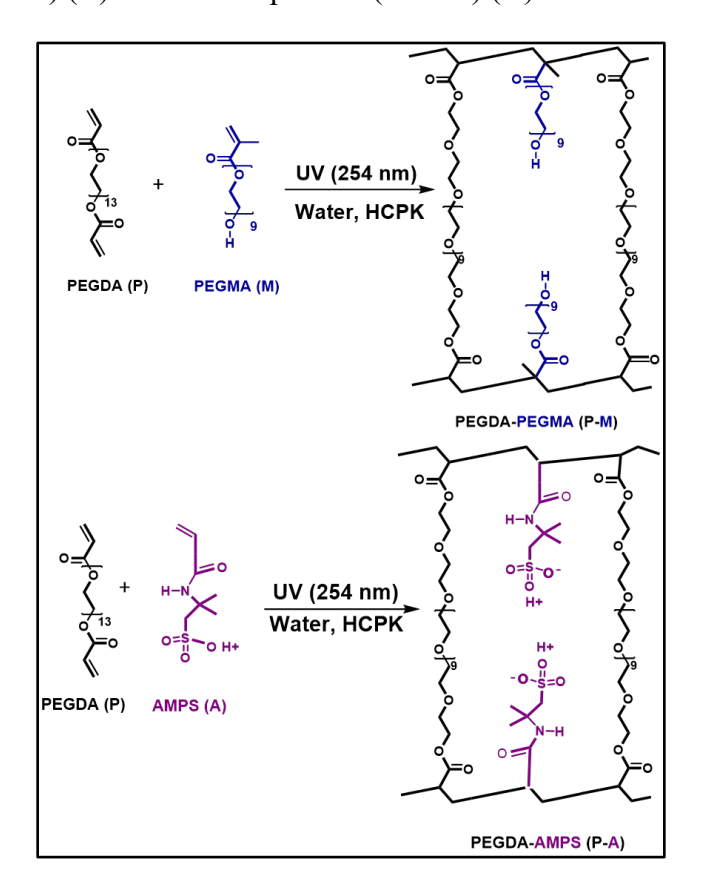


Figure 2: A synthesis scheme of PEGDA, PEGDA-PEGMA, and PEGDA-AMPS membranes.

2. Experimental methods

2.1. Materials

PEGDA (n=13, Mn=700) and PEGMA (n = 9, Mn=500) were purchased from Sigma-Aldrich Chemicals (St. Louis, MS) and Polysciences Inc. (Warrington, PA) respectively. 1-Hydroxylcyclohexyl phenyl ketone (HCPK, photoinitiator) was purchased from Tokyo Chemical Industry (Japan). Sodium carboxylate salts (acetate, formate, propionate, and butanoate) were purchased from ACS Chemical Inc. (Point Pleasant, NJ). Type-1 deionized water produced by a Waterpro BT Purification System from Labconco® (18.2 mΩ cm at 25 °C, 1.2 ppb TOC) (Kansas City, MO) was used in this work. The complete experimental procedure for film formation, physiochemical properties such as water uptake and water volume fraction, ion exchange capacity (IEC), and ionic conductivity measurement for ionic membranes, and the transport experiments such as diffusion cell experiments, and sorption-desorption experiment have been explained in detail in the Supporting Information. The pre-polymerization solution mixture composition of the synthesized membranes have been enlisted in the Table 1.

Table 1. Membrane pre-polymerization mixture (10 g) formulations

	Water ^a	PEGMA ^b	AMPS ^c	PEGDA	PEGMA	AMPS	Water	HCPK
	(wt.%)	(mol%)		(g)	(g)	(g)	(g)	(g)
00-PEGDA	00	00	00	10.00	0.000	0.000	0.000	0.010
10-PEGDA	10	00	00	9.000	0.000	0.000	1.000	0.009
20-PEGDA	20	00	00	8.000	0.000	0.000	2.000	0.008
20-M16	20	16	00	7.042	0.958	0.000	2.000	0.008
20-M32	20	32	00	5.987	2.013	0.000	2.000	0.008
20-A16	20	00	16	7.479	0.000	0.521	2.000	0.008
20-A32	20	00	32	7.022	0.000	0.978	2.000	0.008

^aWater= Weight of Water/ (Weight of Water+ Weight of PEGDA+ Weight of PEGMA) × 100 %

 $^{^{}b}PEGMA = mol\ of\ PEGMA/(mol\ of\ PEGDA + mol\ of\ PEGMA) \times 100\ \%$

 $^{^{}c}AMPS = mol\ of\ AMPS/(mol\ of\ PEGDA + mol\ of\ AMPS) \times 100\ \%$

- 150 XX-PEGDA: XX for pre-polymerization water wt. % with 100 mol% PEGDA.
- 151 XX-MYY: XX for pre-polymerization water wt. %, M for PEGMA, and YY for PEGMA mol%
- 152 XX-AZZ: XX for pre-polymerization water wt. %, A for AMPS, and ZZ for AMPS mol%

3. Results and Discussions:

153

154

155

156

157

158

159

160

161

162

163

164

165

166

167

168

169

170

171

172

In this study, three different series of membranes have been prepared by following the UV-free radical polymerization reaction method. The structure of the three series of membranes has been varied by varying pre-polymerization water from 0 to 20 wt.% (00-PEGDA, 10-PEGDA, 20-PEGDA), varying side chain comonomer PEGMA content from 0 to 32 mol% (e.g. 20-M16, 20-M32), and varying fixed negative charge (AMPS) content from 0 to 32 mol% (20-A16, and 20-A32). The polymer membrane pre-polymerization solution composition for each membrane is provided in Table 1. The homogeneous pre-polymerization solutions and the resulting transparent synthesized membranes indicate relatively homogenous membranes were synthesized¹⁸. The purpose of altering the chemistry of the membranes is to investigate the impact of varying fractional free volume (FFV), adding a side chain pendant comonomer PEGMA group, and an anionic sulfonated fixed charge group AMPS on the permeability of the organic salts of different hydrophobic chain lengths (Na-formate, -acetate, -propionate, and -butanoate). Also, we varied the upstream salt concentrations to elucidate the impact of external salt concentration on transport (permeability, and total ion partition coefficient) through these membranes. The following sections detail the findings from the membrane characterization and membrane transport experiments.

3.1. Water uptake, water volume fraction, ion exchange capacities (IEC), and ionic

conductivity:

PEGDA is an uncharged hydrophilic polyether-based dense/non-porous polymeric membrane having FFV to serve as the passage for the salts/solutes to pass through. To assess the relative

amount of FFV in these membranes, the equilibrium water uptake was characterized. According to Yasuda et al., the free volume in hydrogel membranes proportionally relates to their equilibrium water uptake as diffusion is almost negligible in such hydrogels in their dry state³⁸. The polymer's underlying properties like matrix hydrophilicity, number of charged groups, degree of crosslinking, etc., and external electrolyte solution concentration, with all other conditions held constant (e.g., the type of charged groups and external electrolytes, the interaction between ions and charged groups, etc.) determine the equilibrium water uptake 18,39,40. The water in the hydrogel provides the free volume through which solutes migrate ^{38,41,42}. Hence, we characterized the synthesized membranes by determining the water uptake and water volume fraction by equilibrating the membranes with DI water and aqueous solutions of all four carboxylate salt solutions at varied concentrations. Here, we observe the equilibrium water uptake and water volume fraction increases with increasing water content and AMPS content [see Figure 3, and values are given in Table 1], where increasing pre-polymerization water content has the largest impact on water uptake (and thereby FFV). Meanwhile, the water content is essentially unchanged for increasing PEGMA content (slight increase but within the experimental error), such that subsequent differences in transport behavior discussed below are occurring primarily due to structural differences. In previous work by Ju et al. (2010), a similar pattern was observed where the equilibrium water uptake of PEGDA membranes was increased by increasing prepolymerization water content or adding a side chain pendant comonomer PEGA because of decreasing crosslinking density³⁸. Similarly, our prior work also found this relationship between increasing equilibrium water uptake and water volume fraction and decreasing crosslinking density upon increasing pre-polymerization water content and to a lesser degree comonomer content^{24,25}. Also, in the study by Yan et al. (2018), an increase in the mass fraction of the ionogenic group was

173

174

175

176

177

178

179

180

181

182

183

184

185

186

187

188

189

190

191

192

193

194

found to result in a decrease in the polymer membrane's crosslinking density and ultimately increased water uptake and water volume fraction¹⁸. Overall, a decrease in crosslinking density and an increase in the highly hydrophilic ionogenic groups both contribute to the observed increase in water uptake ^{18,41,42}. Our results here, increased water uptake and water volume fraction upon the addition of sulfonated fixed charge group AMPS are consistent with these prior findings.

Table 2. Water uptake, water volume fraction, ionic conductivity (mS/cm), and ion exchange capacity (IEC) for the range of PEGDA-PEGMA-AMPS water membranes.

	Water Uptake (g/g dry membrane)	Water Volume Fraction (v/v)	Conductivit y (σ, mS/cm)	Theoretical IEC (meq/g dry polymer)	Experiment al IEC (meq/g dry polymer)
00- PEGDA	0.45±0.007	0.352±0.0042		0	0
10- PEGDA	0.63 ± 0.072	0.421±0.0053		0	0
20- PEGDA	0.73±1.020	0.476 ± 0.0097		0	0
20-M16	0.77 ± 0.781	0.478 ± 0.0035		0	0
20-M32	0.84 ± 0.270	0.483 ± 0.0040		0	0
20-A16	0.96 ± 0.020	0.530 ± 0.0090	8.9 ± 0.0004	0.26	0.27
20-A32	0.99±0.670	0.546 ± 0.0008	19.2±0.0500	0.59	0.64

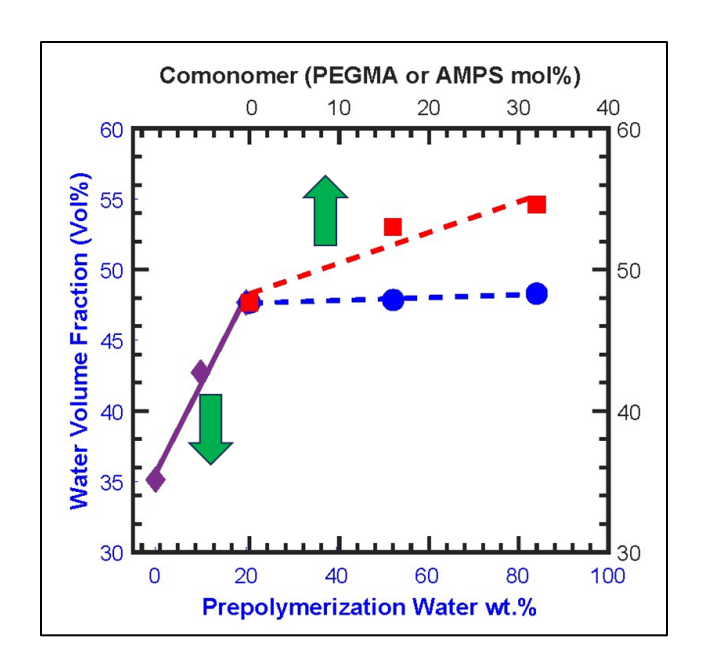


Figure 3: Water volume fractions for polymer films at 0, 10, 20 wt% pre-polymerization water content (♠, solid line), water volume fractions of films at 0, 16, and 32 mol% PEGMA (M) content, prepared with 20 wt.% pre-polymerization water (♠, dashed line) and water volume fractions of films at 0, 16, and 32 mol% AMPS (A) content, prepared with 20 wt.% pre-polymerization water (♠, dashed line) [the upper arrow indicates PEGMA or AMPS mol% as an x-axis variable, and the lower arrow indicates pre-polymerization water wt.% as an x-axis variable].

The results for water volume fraction as a function of each external solute concentration are presented in Figure 4. The dependence of the water volume fraction on each of the external salt solution concentrations is measured for three representatives [20-PEGDA (PEGDA membrane containing 20 wt.% pre-polymerization water), 20-M32 (PEGDA-PEGMA membrane consisting 32 mol% PEGMA and 20 wt.% water), and 20-A32 (PEGDA-AMPS membrane consisting 32 mol% AMPS and 20 wt.% water)] for each of the three different types of synthesized membranes. As the external salt concentration (NaOFm, NaOAc, NaOPr, and NaOBu) increases, the water

volume fraction decreases gradually. The decrease in water volume fraction is attributed to osmotic deswelling which has been observed for other inorganic salts such as NaCl ^{36,37,43,44}. The thermodynamic activity of water in the external solution decreases gradually with increasing salt concentration which leads to a reduction in water volume fraction in the polymeric membranes. It is interesting to note here that the water volume fraction values are highest for the cationic exchange membranes compared to the uncharged membranes; likely due to the higher FFV and presence of ionogenic groups in the membranes containing AMPS. Also, the uncharged membranes without any side chain comonomer (PEGMA or AMPS) show the lowest osmotic deswelling among the three series of membranes [for instance, the osmotic deswelling for sodium formate is around 5% for the membrane composition 20-PEGDA, whereas for 20-A32 the osmotic deswelling is approximately 9%]. We attribute the low osmotic deswelling of 20-PEGDA to a combination of it's lower water volume fraction in pure water and its comparably lower salt solubility (discussed more below) compared to the other films.

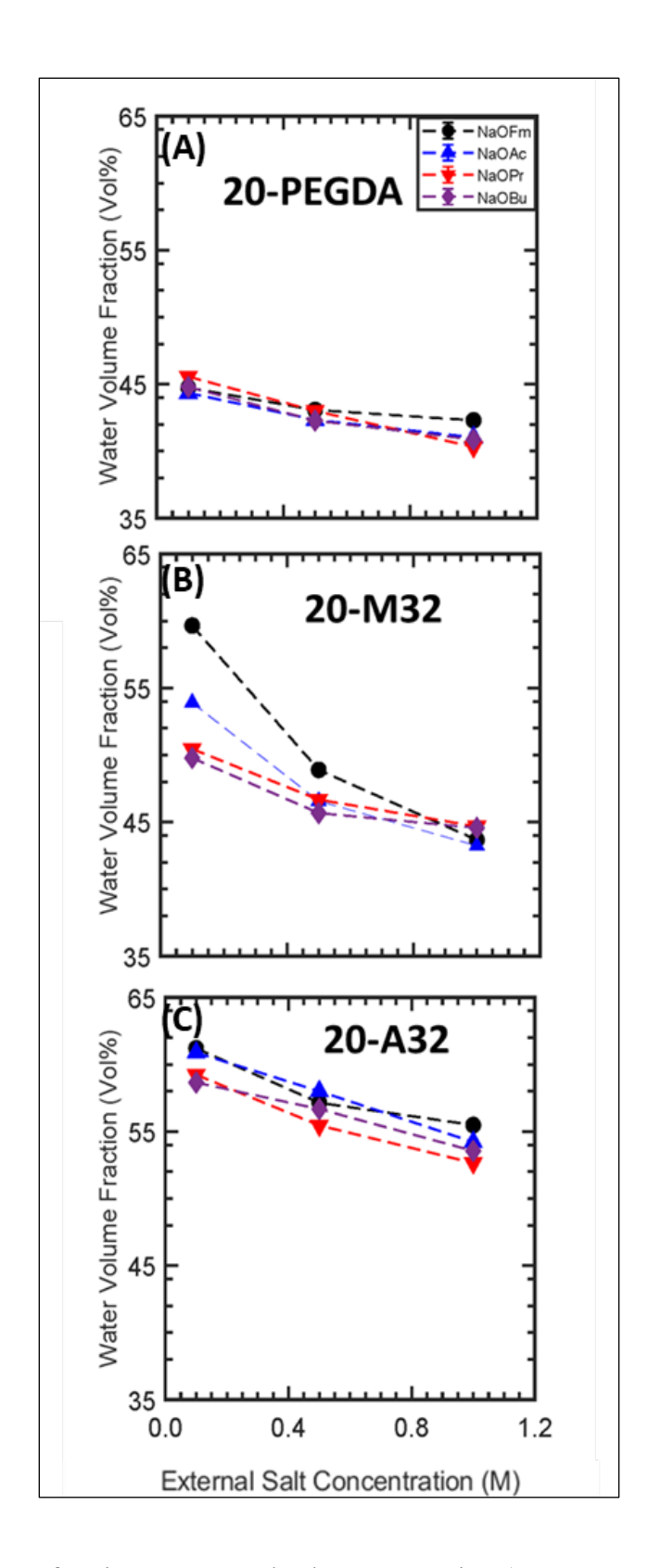


Figure 4: Water volume fraction vs external salt concentration (0,1, 0.5, and 1M).

Ion exchange capacity (IEC) is an essential measurement of the total active sites or functional groups in polymeric ionic films. Here, we used the acid-base titration method to determine IEC [see values in Table 1]. We can see that IEC values increased with the increasing AMPS content from Table 1 as expected for these CEMs (20-A16, and 20-A32) which contain a negative sulfonated charge group (SO₃). For membrane composition with 16 mol% (20-A16), the difference between measured IEC and the theoretical IEC is negligible whereas the difference is approximately 8% for the membrane containing 32 mol% AMPS (20-A32) which is within general expectations.

The in-plane conductivity for the ion-containing membranes was measured utilizing a four-point

conductivity cell. Generally, ionic conductivity is defined as the measure of a membrane's capacity to permit ion transport under the electric field ⁴⁵. The membranes that are employed in electrochemical cells essentially need to be sufficiently conductive to ions to permit current to flow in the device. We performed in-plane conductivity to measure the ionic conductivity for our synthesized CEMs (20-A16, and 20-A32, see Table 1) where the ionic conductivity also increases with the increasing sulfonated charge group (SO₃-) as expected. Generally, ionic conductivity is a function of the volume fraction of the material comprising the conducting phase⁴⁴. Since the sulfonated charge groups are the ion-conducting phase in the synthesized polymeric membranes, the rise in ionic conductivity values with increasing AMPS content is as expected.

3.2. Permeability to carboxylate salts:

We have measured the permeability to four carboxylate salts (sodium formate, acetate, propionate, and butanoate) for three different series of membranes (varying water, varying PEGMA content, and varying AMPS content) at various upstream salt concentrations (0.1, 0.5, and 1M) [See values in Supporting Information Table S1, S2, and S3]. Permeability describes solute transport in a

membrane and is defined as the measured solute flux normalized by the membrane thickness and the driving force for transport. This is influenced by the chemistry and structure of the membrane, the solute, and the solvent, and doesn't depend on the membrane thickness. Here, we performed a diffusion cell experiment to measure the permeability of each salt [see Supporting Information for a detailed experimental procedure] with the results presented in Figure 5.

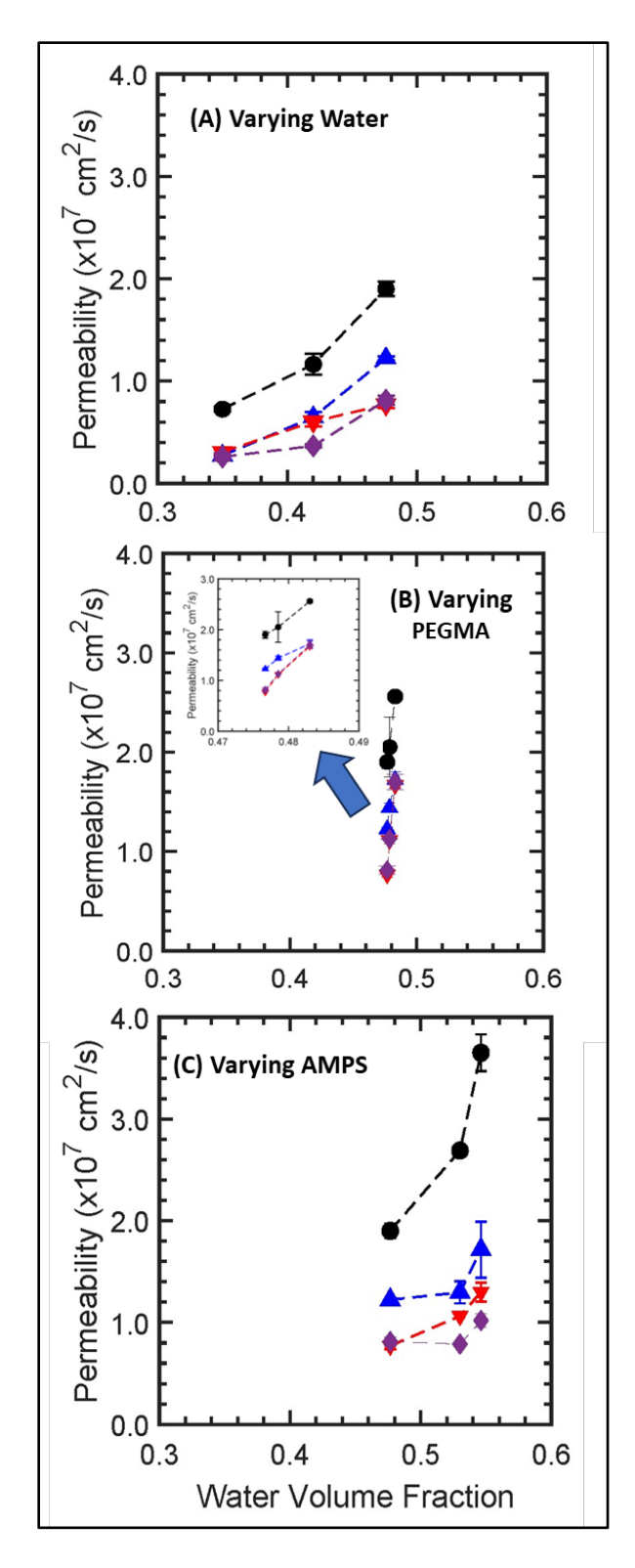


Figure 5: PEGDA-PEGMA-AMPS permeability to NaOFm (●), NaOAc(▲), NaOPr(▼), and NaOBu (◆) in single solute solution vs. water volume fraction (A) at varied pre-polymerization

water content (B) at varied PEGMA content with 20 wt.% pre-polymerization water content, and (C) at varied AMPS content with 20wt.% pre-polymerization water content [Upstream salt concentration 1M] We observe (Figure 5) that the permeability to each salt increases with increasing water volume fraction of the membranes. This behavior is explained by Yasuda et. Al (1971) where water and salt transport through hydrogel-type membranes can be interpreted by the free volume theory of diffusions ^{38,46,47}. Since, in the non-porous/dense membranes, the availability of water channels as the molecular passage for solutes to pass through, the permeability of each salt increases with the increase of water volume fraction. Therefore, increasing water content or AMPS content which both increase water volume fraction leads to corresponding increases in permeability. However, these differences cannot be attributed solely to the water volume fraction, as we also observe large changes in permeability for increasing PEGMA content, which has a relatively negligible impact on water volume fraction. Therefore, for increasing PEGMA content the changes in permeability must be due to changes in the network structure of the film (decrease in crosslink density, faster chain dynamics for pendant PEGMA vs crosslinked PEGDA segments) and the corresponding differences in polymer dynamics and interactions. To start with a broader view, solute transport through uncharged membranes generally occurs due to the presence of the concentration gradient. Though all the salts are transported through the membrane due to the concentration gradient, we find the permeability to sodium formate (NaOFm) is much higher compared to the other three salts. For example, NaOFm's permeability is 1.6 times, 1.2 times, and 1.6 times higher than NaOAc for the compositions 20-PEGDA, 20-M32, and 20-A32. But, for the other three salts (NaOAc, NaOPr, NaOBu), the permeability values are similar, and even overlapped for some compositions, although the permeability to NaOAc is slightly higher than NaOPr, and NaOBu.

267

268

269

270

271

272

273

274

275

276

277

278

279

280

281

282

283

284

285

286

287

288

Previously, our group investigated the single and multicomponent transport of sodium formate, and sodium acetate with either methanol or ethanol and observed the permeability to sodium formate to be higher than that for sodium acetate^{24,25}. It has been interpreted that the hydrated diameter of the formate anion (OFm⁻) is smaller (5.9 Å) than the acetate anion (OAc⁻) (7.44 Å) which led to this higher permeability. We can presume that, with a higher chain length the hydrated diameter increases, and permeability values decrease similarly. Another interesting fact about carboxylate anions is that they have two different kinds of interactions between the salt and the water molecule as most of the carboxylate anions have both hydrophobic and hydrophilic components in the structure. Hydrophobic hydration comes from the molecular structure while hydrophilic (nucleophilic and electrophilic) interactions with water are dominated by electron donor/acceptor atoms and any positively or negatively charged groups present³⁰. Among the carboxylate salts, only sodium formate (NaOFm) is devoid of the hydrophobic group. This different type of attraction between the carboxylate anions and the bulk water plays an important role in bringing the disparity between the inorganic and organic salt transport through the membranes. Ion hydration is an important phenomenon in this respect. According to the study by Rahman et al. (2011), NaOFm and NaOAc irrotationally bind very few water molecules (<2 per anion) on the dielectric relaxation (DR) time scale, although both anions are hydrated as manifested by a significant amount of slow water³¹. Basically, inorganic ions such as CO₃²⁻ irrotationally bind the water molecules around the ions, whereas carboxylate salts fundamentally slow down the dynamics of water molecules adjacent to the ions. This has been termed as slow water in the above-mentioned study. Carboxylate salts can completely immobilize only 1 or 2 water molecules based on prior results from DRS (Dielectric Relaxation Spectroscopy)³¹. In this study, it was found that the effective number of slow water molecules per

290

291

292

293

294

295

296

297

298

299

300

301

302

303

304

305

306

307

308

309

310

311

unit of dissolved salts is approximately 5.2 for OFm⁻³¹. Since OFm⁻ is devoid of the hydrophobic group, these water molecules are connected to the -COO through the H-bond, and according to MD simulations it has been found that the strength of the H-bond is greater than the water-water H-bond which slows the water dynamics around the OFm- salt³¹. It has also been found that the effective number of slow water molecules per unit of dissolved salts for NaOAc is approximately 11, which is much higher than OFm. There are three possible reasons for this: (1) increased hydrophilic hydration of the -COO moiety due to the electron-donating effect of the -CH₃ group; (2) semi-hydrophilic hydration of the -CH₃ moiety, as a result of the polarization of the C-H bonds by the carboxylate group; or (3) hydrophobic hydration of -CH₃³¹. Among these three reasons, the hydrophobicity of the -CH₃ group in OAc contributes to the increasing slow water content which has been validated by different computer simulations, and theoretical considerations³¹. In a follow-up study by Rahman et al. (2012), it was shown that the effective number of slow water molecules per unit of dissolved salts is approximately 23 and 33 respectively for OPr⁻ (aq) and OBu⁻ (aq) which is clearly due to increasing hydrophobic chain length³⁰. Also, hydrophobic interactions were found to smoothly increases with the alkyl chain length³⁰. In a study by Payaka et al. (2010), the CH₃COO-water hydrogen bond was investigated utilizing the QM/MM dynamics⁴⁸. According to this study, there is a strong hydrogen bond between the -COO group and water while the interaction between the hydrogen atom of the -CH₃ group and the nearestneighbor water molecules is comparatively weak ⁴⁸. This leads to the preferential formation of water-water hydrogen bonds instead of hydrogen bonds with the -CH₃ group⁴⁸. Some prior studies note that ions that loosely bind to the surrounding water molecules are in a competitive environment with adjacent water molecules to bind with the polar groups of the polymer chains, eventually lowering permeability compared to cases where the ions are strongly bound to the

313

314

315

316

317

318

319

320

321

322

323

324

325

326

327

328

329

330

331

332

333

334

water molecules ^{49,50}. This explains the much higher permeability of sodium formate compared to the other three carboxylate salts with increasing alkyl chain length observed here. For the higher chain length carboxylate salts, the hydrophobic interactions also begin to play a role leading to the observed decreases in permeability in the case of the other three salts (NaOAc, NaOPr, and NaOBu). For the cation exchange membranes (PEGDA-AMPS), the overall permeability to the carboxylate salts is approximately one order of magnitude less than the permeability to inorganic salts such as 1M NaCl⁵¹. Basically, for highly charged membranes concentration gradient transport is highly impacted by co-ion transport as well³⁷. Here, for each of the carboxylate salts, a common cation is used (Na⁺) and it will inevitably be attracted toward the fixed sulfonated charge group. But still, we can see the decreasing pattern of the permeability with increasing carboxylate anion chain length. This reason is presumably due to Na⁺'s mobility being systematically slowed down (steric hindrance) by the carboxylate anion with the alkyl chain length. We also varied the upstream salt concentrations, 0.1 to 1M [Figure 6], to evaluate the impact on the carboxylate salt transport behavior. In Figure 6, we observe that the permeability to each salt decreases or remains essentially the same with increasing external salt concentration in the case of uncharged membranes. This behavior is like that of other inorganic salt transport through polymeric membranes where it has been found that permeability to salt for uncharged membranes is relatively constant over similar salt concentration ranges^{43,52}. Due to osmotic deswelling the available membrane volume decreases, and so does the permeability which may explain the abovementioned transport behavior. Now, concentrating on the two different series of uncharged membranes, we observe the declining trend is steeper in PEGMA-containing membranes. Relatedly, from Figure 4 we observed the PEGMA-containing membranes osmotically de-swell

336

337

338

339

340

341

342

343

344

345

346

347

348

349

350

351

352

353

354

355

356

357

sharply compared to membranes without PEGMA. From Figure 6, the permeability to NaOAc is much higher than NaOPr, and NaOBu in the membrane that doesn't contain PEGMA [20-PEGDA]. However, the permeability to NaOAc for PEGMA-containing membranes nearly converges with the permeability to NaOPr and NaOBu at 1M salt. It can be presumed that, at 1M concentration, the acetate anion (OAc⁻) faces additional steric hindrance from the PEGMA group, thus the permeability decreases whereas the permeability to NaOPr, and NaOBu is relatively constant throughout the whole concentration range for both series of uncharged membranes. The situation is different for the AMPS-containing membranes, as an increasing trend in permeability with increasing external salt concentration is observed. This increase in permeability to salt with increasing salt concentration has similarly been observed for other membranes and NaCl ^{36,43,44} and can be attributed to impacts from the Donnan exclusion principle. According to this principle, the mobile ion distribution is unequal between the membrane and the solution adjacent to the membrane interface which eventually leads to electric potential (i.e., the Donnan potential) at the membrane/solution interface. This promotes the counterions association with the membrane fixed charge groups and displacement of the co-ions from the membrane interface into the external solution. The Donnan potential usually depends on the difference between the ion concentration in the membrane and the adjacent solution. When the external salt solution is lower in concentration, the Donnan potential increases due to an imbalance in the amount of polymeric fixed charge and counter-ions in the external solution; also, the number of co-ions is lower in the system at lower concentration. Therefore, co-ion sorption is not very pronounced at low concentrations. Whereas, at higher salt concentrations the Donnan potential decreases, and co-ion sorption increases due to the concentration gradient. This explains why overall permeability to salt increases with an increase in upstream salt concentration and the steeper rising trend of

359

360

361

362

363

364

365

366

367

368

369

370

371

372

373

374

375

376

377

378

379

380

permeability to sodium formate with increasing external salt concentration compared to the other three salts as unlike the other three salts NaOFm doesn't have the steric hindrance, and has a smaller hydrated diameter.

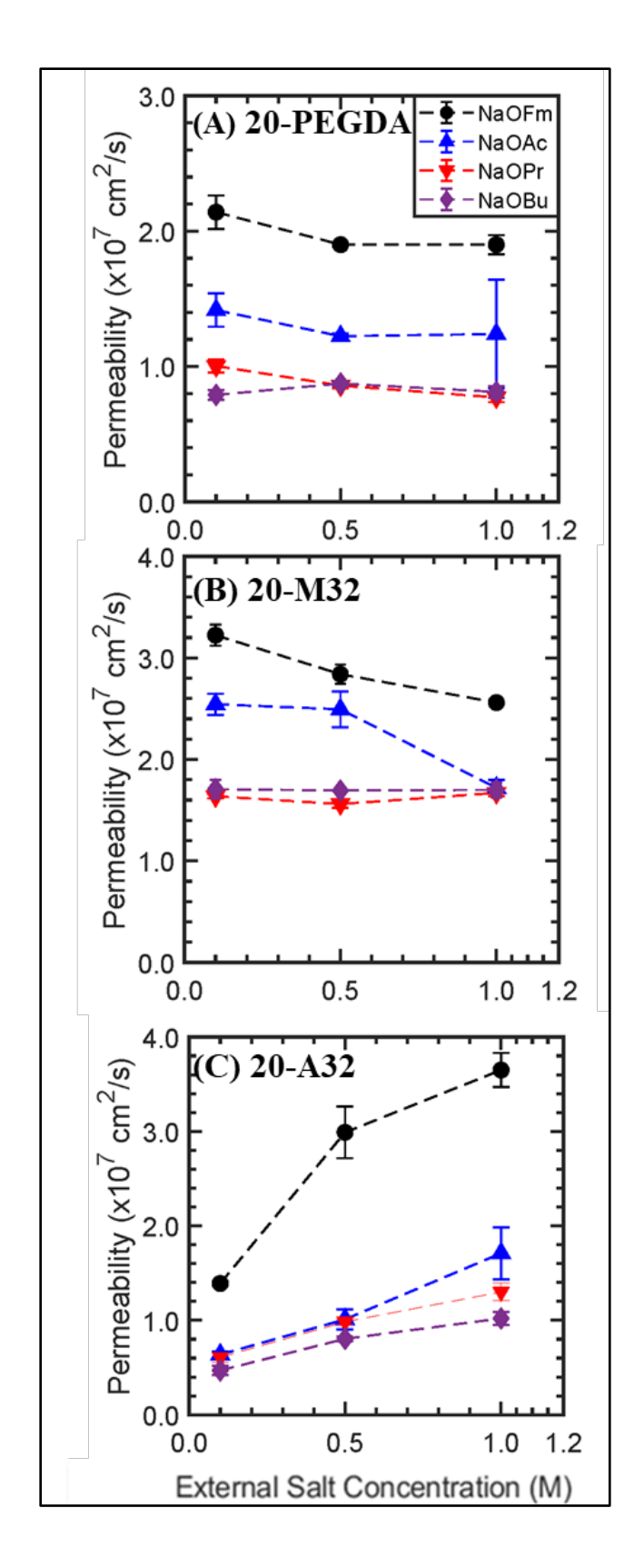


Figure 6: PEGDA-PEGMA-AMPS permeability to NaOFm (●), NaOAc(▲), NaOPr(▼), and NaOBu (◆) in single solute solution vs. external salt concentration for (A) 20-PEGDA (B) 20-M32, and (C) 20-A32.

3.3.Total ion partition coefficient (*K*):

386

387

388

389

390

391

392

393

394

395

396

397

398

399

400

401

402

403

404

405

407

408

The total ion partition coefficient (K) is an important thermodynamic property to characterize solute transport behavior through the membranes which depend on the presence of the fixed charge group in the polymer backbone, external solute concentrations, the interaction between the polymer backbone and the solute, and the type of solute cations and anions. In this study, we performed sorption-desorption experiments to characterize the total ion partition coefficients for the NaOFm, NaOAc, NaOPr, and NaOBu for both the uncharged membranes (PEGDA and PEGMA-containing membranes) and charged membranes (AMPS-containing membranes). Detailed experimental procedures and the resulting values are described in the Supporting Information. Here, we utilized a conductivity meter to measure the ion concentration in the desorption solution. The desorption solution contains all the ions (both the cations and anions) that are desorbed from the membrane surface and the conductivity meter probe tracks the variation of conductivity based on all the ions present in the desorption solution. Here, in this study, the cations are Na⁺ and the anions are formate (OFm⁻), acetate (OAc⁻), propionate (OPr⁻), and butanoate (OBu-). Since we could measure the total desorbed ion concentration from the membrane surface, the total ion partition coefficient (K) of all the carboxylate salts relative to the external solution has been measured here following the Eqn. (1).

$$Ki = \frac{C_i^m}{C_i^s} \tag{1}$$

where C_i^s is the concentration of the solute i in the external solution (0.1, 0.5, and 1 M) and C_i^m is the concentration of the total ions in the film.

Before moving forward towards the discussion of sodium carboxylate salts sorption coefficient for the synthesized membranes, we first postulate how the salt sorption events occurs at the different membrane interfaces. Generally, ion sorption in the uncharged polymer follows the simple ion-partitioning mechanism where ions sorb as mobile salts in the polymer matrix²⁰. For the monovalent salts (1:1 salts), both the cations and anions sorb equally into the uncharged membrane interface to maintain the electroneutrality and the membrane ion concentration increases with the external salt concentration increase 18,20,22,53. Na-Carboxylate salt transport through uncharged and charged membranes is in large part dependent on the interactions between ion-water, water-water, and water-polymer. PEGDA hydration primarily occurs through the polar ether oxygen groups through hydrogen bonding between lone-pair electrons on the ether oxygen groups and the protons of water molecules. The cation (Na⁺) here, is a small, high-charge density ion that tightly bonds to water molecules around their hydration shell and interacts electrostatically with the lone pair electrons on the ether oxygen of the polymer chains disconcerting their hydrogen bond with bulk water⁵⁰. Compared to the Na⁺, the carboxylate anions are large, low-charge density ions interacting weakly with the water molecules. Therefore, the carboxylate anions are believed to be bound with the PEGDA backbone seemingly by a weak non-electrostatic hydrogen bond. However, in charged membranes, there is a disparity between the concentration of cations and anions in the membrane surface based on the ionic fixed groups in the membrane matrix. For example, if the charged polymers have a negative fixed charge group tethered into the polymeric matrix, such as a sulfonated charge group in the AMPS that will attract more counter ions e.g. Na⁺ to electrostatically balance the sulfonated groups tending to the higher cationic concentration than anions due to the "Donnan exclusion principle" described above. Essentially, in the charged membranes (PEGDA-AMPS), the co-ion carboxylate ions are

409

410

411

412

413

414

415

416

417

418

419

420

421

422

423

424

425

426

427

428

429

430

electrostatically repulsed by the sulfonated charge group and the electrostatic repulsion reduces with increased upstream salt concentrations. Also, the anion concentration increases with the external salt concentration due to the decrease of Donnan potential and osmotic deswelling effect (the membrane volume decreases due to osmotic deswelling, and thus the membrane ion concentration rises).

From Figure 7, we see that with an increase in upstream external salt concentration, the total ion concentration in the polymeric membrane matrix increases. If we carefully investigate the Figures 7(A), 7(B), and 7(C), it can be clearly observed that the total ion concentration is lower in the membranes that osmotically deswells the most; such as NaOFm's ion concentration in the 20-PEGDA membrane is ~41% less than in 20-A32 membrane [see Figure 4 for comparing the osmotic deswelling]. Yan et al. (2018) also saw similar behavior in the case of NaCl sorption for PEGDA-AMPS membranes in one of their studies¹⁸.

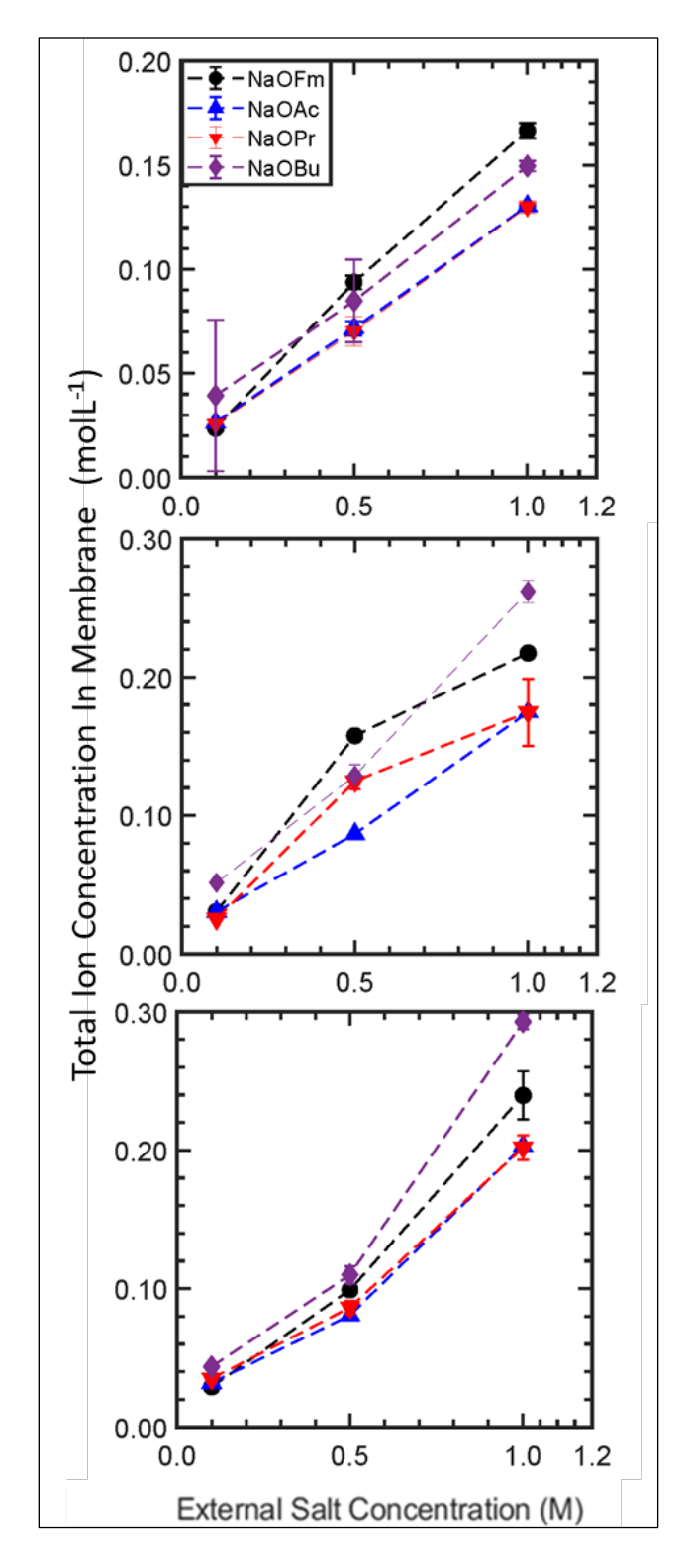


Figure 7: Total ionic concentration of NaOFm (•), NaOAc(△), NaOPr(▼), and NaOBu (•) in the membrane vs. external salt concentration for (A) 20-PEGDA (B) 20-M32, and (C) 20-A32.

Now, we discuss the total ion partition coefficient of each Na-carboxylate salt at the membrane surface based on the variation of membrane chemistry and external salt concentration in this section [Table S4, S5, and S6]. Previously it has been mentioned that three different series of membranes have been synthesized for the current study and they are varied by varying (a) prepolymerization water content; (b) varying PEGMA content, and (c) varying AMPS content. From Figure 8(A), it can be noticed that the total partition coefficient (K) for all the carboxylate salts is increasing with the variation of pre-polymerization water content. Similar behavior has been observed in prior studies^{18,25,50}. For example, Yan et al. (2022), performed an ion sorption study for NaCl in PEGDA-AMPS membranes and observed the ion sorption coefficient for NaCl decreases in the membranes with lower water volume fraction⁵⁴. Essentially, the ethylene oxide (EO) groups in the PEGDA backbone are likely to compete for water molecules with the sorbed ions. Thus, the availability of water for ion solvation lessens, and eventually that reduces ionsorption. Here, all the carboxylate salts demonstrated identical sorption behavior through PEGDA membranes with various water volume fractions. Also, from Figure 8(B) where we have varied the membrane chemistry by varying side chain comonomer PEGMA, we saw total ion partition coefficients for all the carboxylate salts increased with the variation of PEGMA content. Also, the total ion partition coefficient values are seemingly higher in the PEGMA containing membranes than the other three. The reason may be due to additional interactions between the PEGMA EO groups and the hydrated carboxylate salts (having additional water molecules by adding PEGMA to solvate the salts. This would explain the variation in carboxylate salts permeability through the membranes even with negligible difference in water volume fraction with increasing PEGMA content.

447

448

449

450

451

452

453

454

455

456

457

458

459

460

461

462

463

464

465

466

467

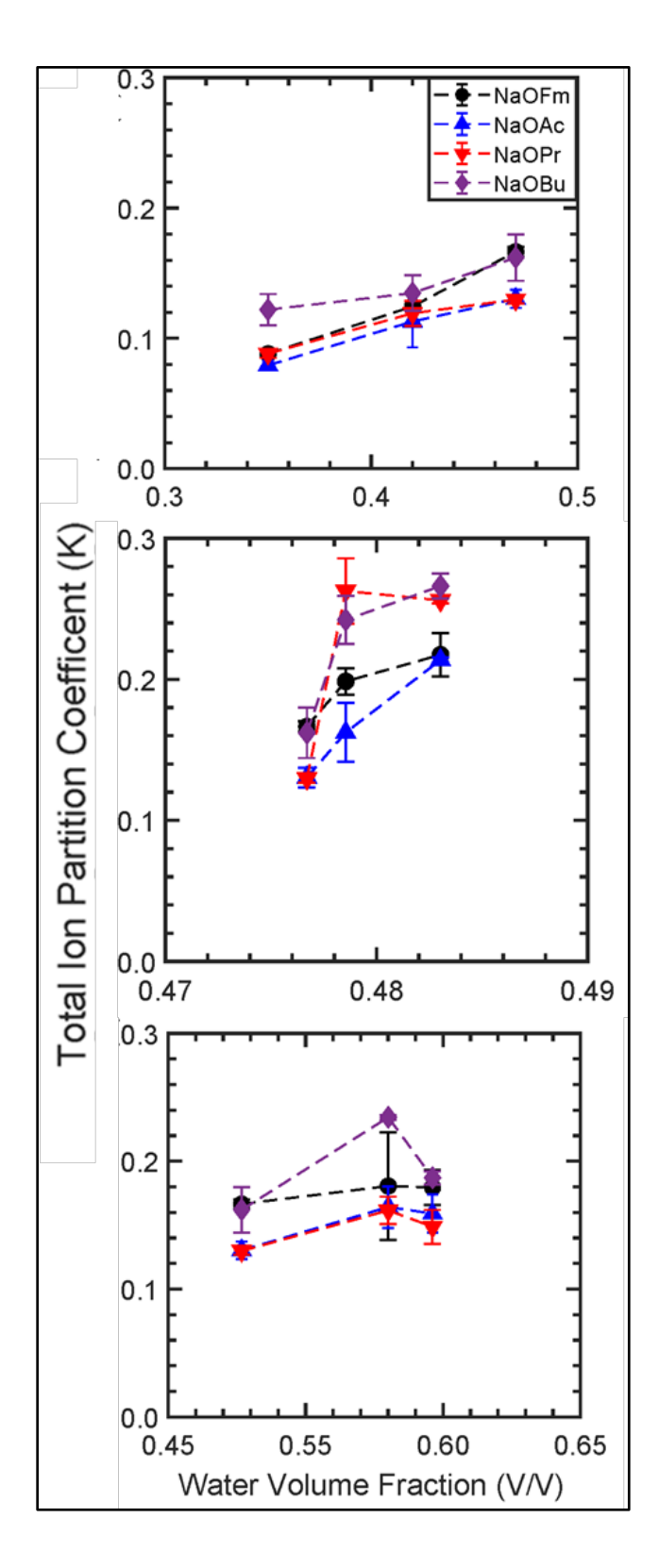


Figure 8: Total Partition Coefficient of PEGDA-PEGMA-AMPS to NaOFm (●), NaOAc(▲), NaOPr(▼), and NaOBu (◆) in single solute solution vs. water volume fraction for (A)varying pre-polymerization water wt.% (B) varying PEGMA mol%, and (C) varying AMPS mol%.

473

474

475

476

477

478

479

480

481

482

483

484

485

486

487

488

489

490

491

492

470

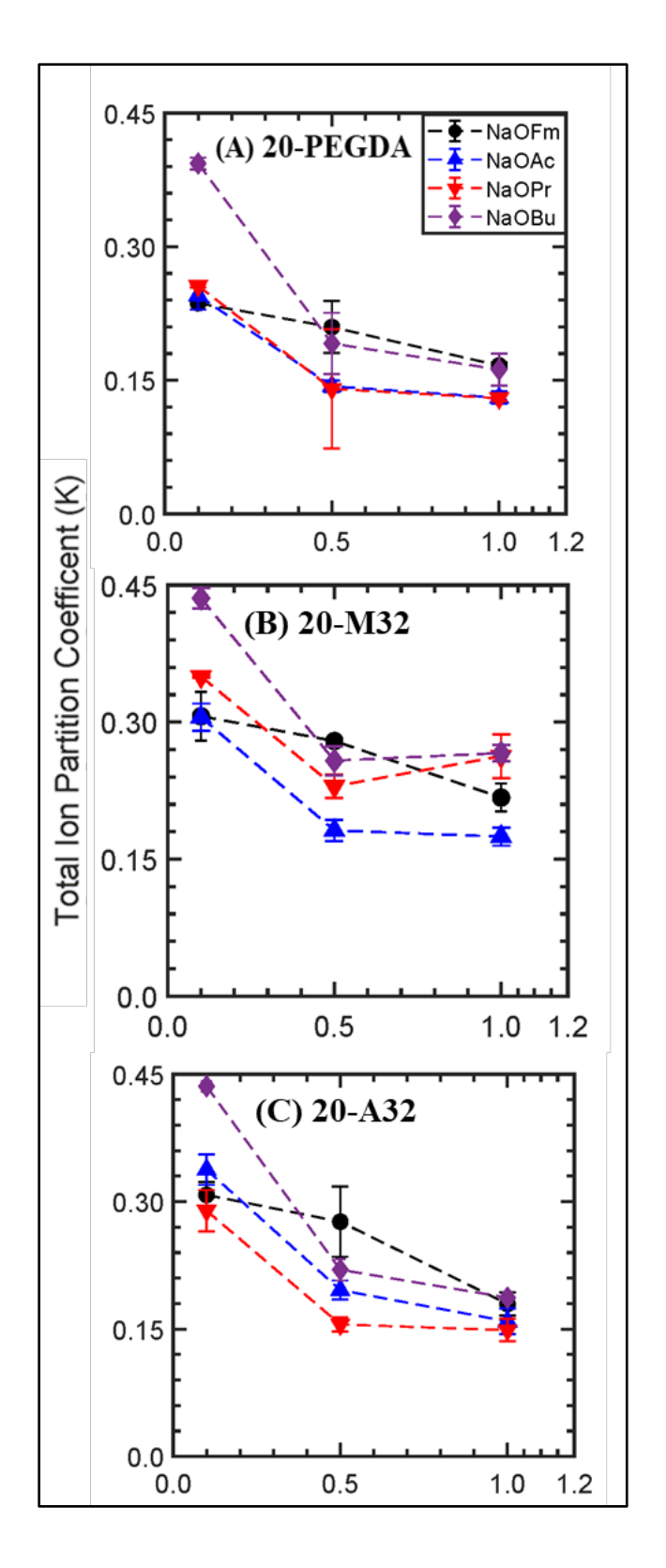
471

472

Now, we examine how the total ion partition coefficient varies against membrane water volume fraction for the AMPS-containing membranes. Although the total ion partition coefficient increases for the 16 mol% AMPS (relative to PEGDA) which could be explained by the increase of water volume fraction in the membrane due to the increase in AMPS content, a downturn of the total ion partition coefficient is observed from the 16 to 32 mol% AMPS [total ion partition coefficient of NaOFm, NaOAc, NaPr, and NaOBu decreased 5.66%, 6.25%, 8.07%, and 21% respectively]. With the increase of sulfonated charge group AMPS, the distinction between the negative sulfonated charge group and carboxylate anions due to the "Donnan Exclusion" principle becomes more pronounced which is the probable cause of the above-mentioned behavior ^{18,25,55}. The total ion partition co-efficient for three representative membranes from the three series (20-PEGDA, 20-M32, and 20-A32) with varied upstream carboxylate salt concentration variation will be considered. We see from Figure 9 that, for the membrane composition 20-PEGDA, and 20-M32 membranes the total ion partition coefficient for NaOFm, NaOAc, NaOPr, and NaOBu decreases from 0.1 to 0.5 M, and remains almost the same from 0.5 to 1M, but decreases gradually with increasing concentration for the membrane composition 20-A32. Analogous behavior has been exhibited by Wang et al. (2023) while describing the significance of co-ion partitioning in salt transport through polyamide reverse osmosis membrane which contained a negative charge in the backbone. In that study, quartz crystal microbalance was used to measure the salt partitioning through polyamide membranes, where NaCl was the model salt, and it was observed that the total ion partitioning coefficient decreases with increasing upstream salt concentration. Some other prior studies also saw a similar kind of trend ^{56,57}, and Wang et al. explained this behavior as another consequence of the "Donan Exclusion" principle but the salt partitioning in the membrane was modified from the classic Donnan theory (for monovalent salts) to derive the following Eqn.

$$K_{total} = \Phi \cosh \left(\Delta \Phi_{D} \right) \tag{2}$$

where K_{total} is the total ion partition coefficient; Φ is the non-Donnan partitioning coefficient (the geometric mean of Φ ct and Φ co), and $\Delta\Phi_D$ is the dimensionless Donnan potential⁵⁸. With an increase in external salt concentration, the Donnan potential between the membrane surface and the external salt solution diminishes, therefore, the total ion partition coefficient decreases gradually in the charged membranes (20-A32) [Figure 9(C)]. Apart from the Donnan partitioning of the salts at the membrane surface, there is also a non-electrostatic salt partition as well which is called a non-Donnan effect. This non-Donnan effect does depend on the pore and ion size but is independent of salt concentration. This may play a role in the almost flat trend of the total partition coefficient from 0.5 to 1M in the case of the charge-neutral membranes 20-PEGDA, and 20-M32 [Figure 9(A), and 9(B)].



NaOPr(♥), and NaOBu (♦) in single solute solution vs. external salt concentration for (A) 20-PEGDA (B) 20-M32, and (C) 20-A32. Although the total ion partition coefficient doesn't govern salt permeability, we will still investigate comparing the values of the four carboxylate salts sorption coefficients here. For example, at 0.1 M upstream salt concentration, for the membrane composition 20-PEGDA, the total partition coefficient for NaOFm, NaOAc, NaOPr, and NaOBu is 0.23, 0.25, 0.26, and 0.39 respectively; for the membrane composition 20-PEGDA, the total partition coefficient for NaOFm, NaOAc, NaOPr, and NaOBu is 0.31, 0.29, 0.35, and 0.52 respectively; and for the membrane composition 20-A32, the total partition coefficient for NaOFm, NaOAc, NaOPr, and NaOBu is 0.31, 0.34, 0.29, and 0.44. Here, we can see that NaOBu's total partition coefficient is greater than all the other three solutes at 0.1 M upstream salt concentration (for instance, NaOBu's total partition coefficient is 67%, 79%, 48% larger than NaOFm, NaOAc, and NaOPr respectively for 20-PEGDA). However, the total partition coefficients of NaOFm, NaOAc, and NaOPr are not significantly different from each other at that concentration. However, the differences among the partition coefficients reduce with an increase in solute concentrations. Since, in this study, the only cation is Na⁺, we assume that the solubility values differed based on the different anions (the carboxylates). According to the dielectric relaxation spectroscopy (DRS), with the increase of alkyl chain length, the hydrophobic interaction of the salts increases. Thus, the number of bound water molecules increases with the increasing hydrophobic chain length and so does the hydration of the molecules. Also, hydrophobic interaction reduces with the increase of high salt concentration^{30,31}. That might explain NaOBu's visibly higher total partition coefficient compared to the other three salts having the highest number of hydrophobic alkyl chain lengths at 0.1 M

Figure 9: Total partition coefficient of PEGDA-PEGMA-AMPS to NaOFm (●), NaOAc(△),

510

511

512

513

514

515

516

517

518

519

520

521

522

523

524

525

526

527

528

529

530

531

concentration which reduced with the upstream salt concentration and merges with the other three Therefore, we can conjecture that the electrostatic repulsion might be lowest in the case of carboxylate salts with a large number of alkyl chain lengths due to additional hydrophobic interaction with the polymer. On the other hand, if we refer to Figure 6 for the permeability values, we can see that NaOFm's permeability is the largest among all three salts, and decreases based on increasing carboxylate chain length in the whole range of upstream salt concentrations. This points to the transport of carboxylate salts through the membranes being mostly dependent on diffusivity or kinetic parameters rather than the thermodynamic parameters due to the similarity in the partition coefficients.

3.4.Diffusivity:

Solute diffusivity through the membranes is associated with the polymer structure (the size and amount of fractional free volume in the membranes) and the solute's molecular size. According to Yasuda et al. $(1971)^{46}$ the free volume in hydrated polymers is proportional to the volume fraction of water in the polymers and the solute diffusivity in the water-swollen polymer, D_i , is dependent on the free volume, v_f , as Eqn. (3)

$$D_i \propto \exp\left(-\frac{\nu^*}{\nu_f}\right) \tag{3}$$

where ν^* is the minimum size of a free volume element to diffuse a solute. As membrane-free volume is proportional to the volume fraction of water, ϕ_w , Eqn. (3) can be expressed by Eq. (4)

$$D_i = D_{o,i} \exp\left(-A\left(\frac{1}{\phi_w} - 1\right)\right) \tag{4}$$

where $D_{o,i}$ is the solute diffusivity in water, and A is an empirical constant.

Solute diffusivities can thereby be calculated utilizing the solution diffusion model equation $(P=K\times D)$, and permeability and sorption coefficient data. Although co-ion partition or co-ion sorption coefficients are generally utilized to calculate the diffusivity values; here we have plugged the total sorption coefficients determined from the total ion concentration (both cation and anions together) into the solution-diffusion model to calculate the diffusivity values discussed here. The assumption is that since the cation is common for the four salts (Na⁺), the relative differences among the sorption coefficient values are coming from the variation of anions. In Figure 10, we have shown the diffusivity values for varied compositions at 1M upstream salt concentrations. The increasing diffusivity values for all the solutes with increasing water volume fractions can be explained by the equation described at Eqn. (3) and Eqn. (4). We can see that the smallest increase in diffusivity values is observed for variation of PEGMA content since PEGMA has a negligible impact on fractional free volume (as judged by water volume fraction). If we carefully compare the diffusivity values from Figure 10, we can see that they vary solely based on their hydrated molecular structural fluctuation and this is the similar pattern that has been reflected on the permeability results at Figure 5.

553

554

555

556

557

558

559

560

561

562

563

564

565

566

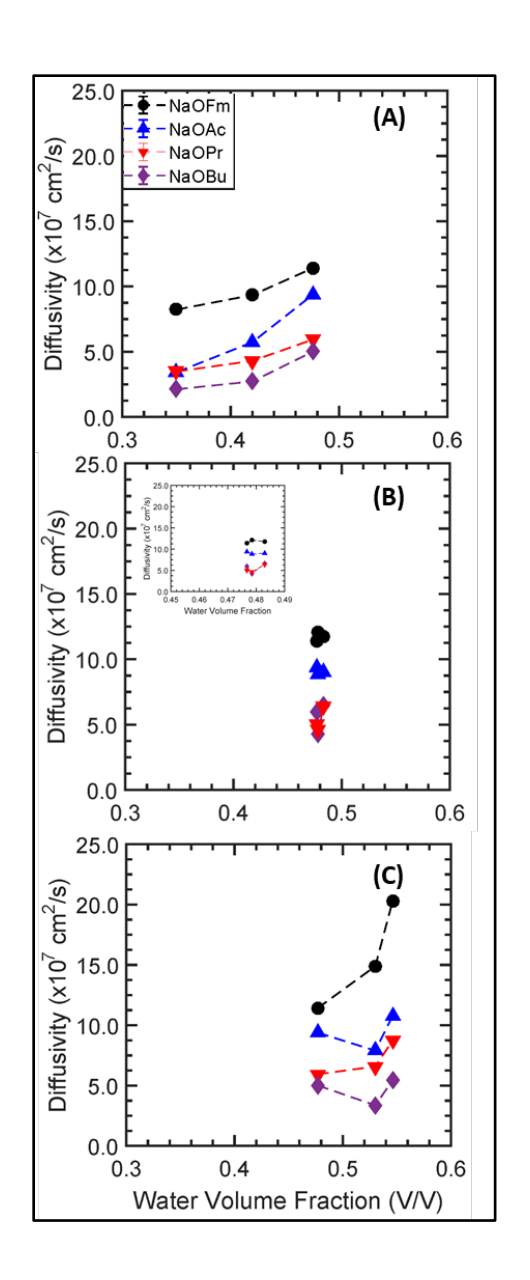


Figure 10: PEGDA-PEGMA-AMPS's diffusivity to NaOFm (●), NaOAc(▲), NaOPr (▼), and NaOBu (♠) in single solute solution vs. water volume fraction (A) at varied pre-polymerization water content (B) at varied PEGMA content with 20 wt.% pre-polymerization water content, and (C) at varied AMPS content with 20wt.% pre-polymerization water content [upstream salt concentration 1M]

By comparing the values for both total partition co-efficient and diffusivity values measured at 1M upstream salt concentration for all the compositions, we deduce that, kinetics is the major factor for governing transport of carboxylate salts through most of the polyether based-membranes.

577

578

579

580

581

582

583

584

585

586

587

588

589

590

591

592

593

594

595

596

574

575

576

4. Conclusions:

This study investigated the transport behavior of carboxylate salts of increasing hydrophobic chain length through three series of varying PEGDA-based membranes with 1) varying prepolymerization water content; 2) varying uncharged side chain comonomer PEGMA, and 3) varying charged comonomer AMPS. Here, four model sodium carboxylate salts with increasing hydrophobic chain length (NaOFm, NaOAc, NaOPr, and NaOBu) were chosen as the solutes and their transport and sorption behavior characterized for three upstream solute concentrations (0.1 to 1 M). Although the basic transport pattern for all the carboxylate salts follows a similar trend to other monovalent salts such as NaCl for all the membrane chemistries, distinct behavior is observed for the carboxylate salts based on the different membrane structures. The permeability of the membranes to the carboxylate salts are smaller overall than the other inorganic monovalent salts presumably due to the inability to effectively immobilize the water molecules around the salts and steric hindrance from the larger carboxylate ions. While the order of increasing permeability is NaOFm>NaOAC >NaOPr ≥ NaOBu through most of the membrane chemistries, we observed the permeability to NaOAc nearly converges with NaOPr and NaOBu permeability at higher salt concentrations (1M). We also observe the permeability to NaOFm is much higher than the other three carboxylate salts for all the membrane chemistries which we attribute to the absence of a hydrophobic chain. Another interesting factor is in comparing the total partition coefficients among the carboxylate salts, where while the permeability to NaOBu is much higher than the other

three salts, at the higher upstream salt concentration (1M) the total partition coefficient values converge. From this, we can conclude that the carboxylate salt transport dynamics through these PEGDA-based dense membranes are primarily governed by kinetics rather than thermodynamics (sorption). This is useful for informing the molecular design of both uncharged and ion exchange membranes for applications such as CO₂ reduction cells, or membrane-based bio reactors dealing with VFAs (volatile fatty acids) as tailoring the design to either limit or improve kinetic aspects may prove fruitful even if they occur at the expense of anticipated or desired sorption behavior.

604

605

606

607

608

609

597

598

599

600

601

602

603

Acknowledgments: This material is based upon work supported by the National Science Foundation under Grant No. 1936146. AH also acknowledges support by the National Science Foundation under Grant No. 1950304. Any opinions, findings, and conclusions or recommendations expressed in this material are those of the author(s) and do not necessarily reflect the views of the National Science Foundation."

610

References:

- 613 (1) Khan, M. H.; Akash, N. M.; Akter, S.; Rukh, M.; Nzediegwu, C.; Islam, M. S. A
- 614 Comprehensive Review of Coconut-Based Porous Materials for Wastewater Treatment and CO2
- 615 Capture. J. Environ. Manag. 2023, 338, 117825. https://doi.org/10.1016/j.jenvman.2023.117825.
- 616 (2) Brody, L.; Rukh, M.; Cai, R.; Bosari, A. S.; Schomäcker, R.; Li, F. Sorption-Enhanced Steam
- Reforming of Toluene Using Multifunctional Perovskite Phase Transition Sorbents in a
- 618 Chemical Looping Scheme. J. Phys.: Energy **2023**, 5 (3), 035004. https://doi.org/10.1088/2515-
- 619 7655/acdbe9.
- 620 (3) Olivares-Marín, M.; Maroto-Valer, M. M. Development of Adsorbents for CO2 Capture from
- Waste Materials: A Review. Greenh. Gases: Sci. Technol. 2012, 2 (1), 20–35.
- 622 https://doi.org/10.1002/ghg.45.
- 623 (4) Evans, C. M.; Sanoja, G. E.; Popere, B. C.; Segalman, R. A. Anhydrous Proton Transport in
- Polymerized Ionic Liquid Block Copolymers: Roles of Block Length, Ionic Content, and

- 625 Confinement. *Macromolecules* **2016**, *49* (1), 395–404.
- 626 https://doi.org/10.1021/acs.macromol.5b02202.
- 627 (5) Singh, M. R.; Clark, E. L.; Bell, A. T. Effects of Electrolyte, Catalyst, and Membrane
- 628 Composition and Operating Conditions on the Performance of Solar-Driven Electrochemical
- 629 Reduction of Carbon Dioxide. *Phys Chem Chem Phys* **2015**, *17* (29), 18924–18936.
- 630 <u>https://doi.org/10.1039/c5cp03283k.</u>
- 631 (6) Liang, S.; Altaf, N.; Huang, L.; Gao, Y.; Wang, Q. Electrolytic Cell Design for
- 632 Electrochemical CO2 Reduction. *J Co2 Util* **2020**, *35*, 90–105.
- 633 <u>https://doi.org/10.1016/j.jcou.2019.09.007</u>.
- 634 (7) Chabi, S.; Papadantonakis, K. M.; Lewis, N. S.; Freund, M. S. Membranes for Artificial
- 635 Photosynthesis. *Energ Environ Sci* **2017**, *10* (6), 1320–1338.
- 636 <u>https://doi.org/10.1039/c7ee00294g</u>.
- 637 (8) Krödel, M.; Carter, B. M.; Rall, D.; Lohaus, J.; Wessling, M.; Miller, D. J. Rational Design
- of Ion Exchange Membrane Material Properties Limits the Crossover of CO2 Reduction
- Products in Artificial Photosynthesis Devices. Acs Appl Mater Inter 2020, 12 (10), 12030–
- 640 12042. https://doi.org/10.1021/acsami.9b21415.
- 641 (9) Lim, R. J.; Xie, M.; Sk, M. A.; Lee, J.-M.; Fisher, A.; Wang, X.; Lim, K. H. A Review on the
- Electrochemical Reduction of CO2 in Fuel Cells, Metal Electrodes and Molecular Catalysts.
- 643 *Catal Today* **2014**, *233*, 169–180. https://doi.org/10.1016/j.cattod.2013.11.037.
- 644 (10) Luo, T.; Abdu, S.; Wessling, M. Selectivity of Ion Exchange Membranes: A Review. J
- 645 *Membrane Sci* **2018**, *555*, 429–454. https://doi.org/10.1016/j.memsci.2018.03.051.
- 646 (11) Wu, J.; Huang, Y.; Ye, W.; Li, Y. CO2 Reduction: From the Electrochemical to
- 647 Photochemical Approach. *Adv Sci* **2017**, *4* (11), 1700194.
- 648 https://doi.org/10.1002/advs.201700194.
- 649 (12) Garza, A. J.; Bell, A. T.; Head-Gordon, M. Mechanism of CO2 Reduction at Copper
- 650 Surfaces: Pathways to C2 Products. *Acs Catal* **2018**, 8 (2), 1490–1499.
- 651 https://doi.org/10.1021/acscatal.7b03477.
- 652 (13) Kuhl, K. P.; Cave, E. R.; Abram, D. N.; Jaramillo, T. F. New Insights into the
- Electrochemical Reduction of Carbon Dioxide on Metallic Copper Surfaces. *Energ Environ Sci*
- **2012**, *5* (5), 7050–7059. https://doi.org/10.1039/c2ee21234j.
- 655 (14) Lee, A.; Elam, J. W.; Darling, S. B. Membrane Materials for Water Purification: Design,
- 656 Development, and Application. Environ Sci Water Res Technology 2015, 2 (1), 17–42.
- 657 https://doi.org/10.1039/c5ew00159e.
- 658 (15) Crothers, A. R.; Darling, R. M.; Kushner, D. I.; Perry, M. L.; Weber, A. Z. Theory of
- Multicomponent Phenomena in Cation-Exchange Membranes: Part III. Transport in Vanadium

- Redox-Flow-Battery Separators. J Electrochem Soc 2020, 167 (1), 013549.
- 661 https://doi.org/10.1149/1945-7111/ab6725.
- 662 (16) Grzegorzek, M.; Majewska-Nowak, K.; Ahmed, A. E. Removal of Fluoride from
- Multicomponent Water Solutions with the Use of Monovalent Selective Ion-Exchange
- 664 Membranes. Sci Total Environ **2020**, 722, 137681.
- 665 <u>https://doi.org/10.1016/j.scitotenv.2020.137681</u>.
- 666 (17) Benvenuti, T.; García-Gabaldón, M.; Ortega, E. M.; Rodrigues, M. A. S.; Bernardes, A. M.;
- Pérez-Herranz, V.; Zoppas-Ferreira, J. Influence of the Co-Ions on the Transport of Sulfate
- through Anion Exchange Membranes. *J Membrane Sci* **2017**, *542*, 320–328.
- 669 <u>https://doi.org/10.1016/j.memsci.2017.08.021.</u>
- 670 (18) Yan, N.; Paul, D. R.; Freeman, B. D. Water and Ion Sorption in a Series of Cross-Linked
- 671 AMPS/PEGDA Hydrogel Membranes. *Polymer* **2018**, *146*, 196–208.
- 672 https://doi.org/10.1016/j.polymer.2018.05.021.
- 673 (19) Sarapulova, V. V.; Titorova, V. D.; Nikonenko, V. V.; Pismenskaya, N. D. Transport
- 674 Characteristics of Homogeneous and Heterogeneous Ion-Exchange Membranes in Sodium
- 675 Chloride, Calcium Chloride, and Sodium Sulfate Solutions. Membr Membr Technologies 2019, 1
- 676 (3), 168–182. https://doi.org/10.1134/s2517751619030041.
- 677 (20) Geise, G. M.; Paul, D. R.; Freeman, B. D. Fundamental Water and Salt Transport Properties
- of Polymeric Materials. *Prog Polym Sci* **2014**, *39* (1), 1–42.
- 679 https://doi.org/10.1016/j.progpolymsci.2013.07.001.
- 680 (21) Kingsbury, R. S.; Wang, J.; Coronell, O. Comparison of Water and Salt Transport
- Properties of Ion Exchange, Reverse Osmosis, and Nanofiltration Membranes for Desalination
- and Energy Applications. *J Membrane Sci* **2020**, *604*, 117998.
- 683 https://doi.org/10.1016/j.memsci.2020.117998.
- 684 (22) Geise, G. M.; Cassady, H. J.; Paul, D. R.; Logan, B. E.; Hickner, M. A. Specific Ion Effects
- on Membrane Potential and the Permselectivity of Ion Exchange Membranes. *Phys Chem Chem*
- 686 Phys **2014**, 16 (39), 21673–21681. https://doi.org/10.1039/c4cp03076a.
- 687 (23) Kim, J. M.; Beckingham, B. S. Comonomer Effects on Co-Permeation of Methanol and
- Acetate in Cation Exchange Membranes. Eur Polym J 2021, 147, 110307.
- 689 https://doi.org/10.1016/j.eurpolymj.2021.110307.
- 690 (24) Mazumder, A.; Kim, J. M.; Hunter, B.; Beckingham, B. S. Controlling Fractional Free
- Volume, Transport, and Co-Transport of Alcohols and Carboxylate Salts in PEGDA Membranes.
- 692 *Membr* **2022**, *13* (1), 17. https://doi.org/10.3390/membranes13010017.
- 693 (25) Kim, J. M.; Mazumder, A.; Li, J.; Jiang, Z.; Beckingham, B. S. Impact of PEGMA on
- Transport and Co-Transport of Methanol and Acetate in PEGDA-AMPS Cation Exchange
- 695 Membranes. J Membrane Sci 2022, 642, 119950. https://doi.org/10.1016/j.memsci.2021.119950.

- 696 (26) Dobyns, B. M.; Kim, J. M.; Li, J.; Jiang, Z.; Beckingham, B. S. Multicomponent Transport
- of Alcohols in Nafion 117 Measured by in Situ ATR FTIR Spectroscopy. *Polymer* **2020**, *209*,
- 698 123046. https://doi.org/10.1016/j.polymer.2020.123046.
- 699 (27) Kim, J. M.; Dobyns, B. M.; Zhao, R.; Beckingham, B. S. Multicomponent Transport of
- 700 Methanol and Acetate in a Series of Crosslinked PEGDA-AMPS Cation Exchange Membranes.
- 701 J Membrane Sci **2020**, 614, 118486. https://doi.org/10.1016/j.memsci.2020.118486.
- 702 (28) Dobyns, B. M.; Kim, J. M.; Beckingham, B. S. Multicomponent Transport of Methanol and
- 703 Sodium Acetate in Poly(Ethylene Glycol) Diacrylate Membranes of Varied Fractional Free
- Volume. Eur Polym J **2020**, 134, 109809. https://doi.org/10.1016/j.eurpolymj.2020.109809.
- 705 (29) Kim, J. M.; Beckingham, B. S. Transport and Co-transport of Carboxylate Ions and
- Alcohols in Cation Exchange Membranes. J Polym Sci 2021, 59 (21), 2545–2558.
- 707 <u>https://doi.org/10.1002/pol.20210383</u>.
- 708 (30) Rahman, H. M. A.; Hefter, G.; Buchner, R. Hydrophilic and Hydrophobic Hydration of
- Sodium Propanoate and Sodium Butanoate in Aqueous Solution. J Phys Chem B 2013, 117 (7),
- 710 2142–2152. https://doi.org/10.1021/jp310029c.
- 711 (31) Rahman, H. M. A.; Hefter, G.; Buchner, R. Hydration of Formate and Acetate Ions by
- 712 Dielectric Relaxation Spectroscopy. J Phys Chem B 2012, 116 (1), 314–323.
- 713 https://doi.org/10.1021/jp207504d.
- 714 (32) Gojło, E.; Śmiechowski, M.; Panuszko, A.; Stangret, J. Hydration of Carboxylate Anions:
- 715 Infrared Spectroscopy of Aqueous Solutions. J Phys Chem B 2009, 113 (23), 8128–8136.
- 716 https://doi.org/10.1021/jp811346x.
- 717 (33) Kameda, Y.; Fukuhara, K.; Mochiduki, K.; Naganuma, H.; Usuki, T.; Uemura, O. Structure
- of HCOOK Hydrated Melts. J Non-cryst Solids 2002, 312, 433–437.
- 719 https://doi.org/10.1016/s0022-3093(02)01706-4.
- 720 (34) Jorgensen, W. L.; Gao, J. Monte Carlo Simulations of the Hydration of Ammonium and
- 721 Carboxylate Ions. *J Phys Chem* **1986**, *90* (10), 2174–2182. https://doi.org/10.1021/j100401a037.
- 722 (35) Fan, H.; Huang, Y.; Yip, N. Y. Advancing Ion-Exchange Membranes to Ion-Selective
- Membranes: Principles, Status, and Opportunities. Front Env Sci Eng 2023, 17 (2), 25.
- 724 https://doi.org/10.1007/s11783-023-1625-0.
- 725 (36) Kamcey, J.; Galizia, M.; Benedetti, F. M.; Jang, E.-S.; Paul, D. R.; Freeman, B. D.;
- Manning, G. S. Partitioning of Mobile Ions between Ion Exchange Polymers and Aqueous Salt
- Solutions: Importance of Counter-Ion Condensation. Phys Chem Chem Phys **2016**, 18 (8), 6021–
- 728 6031. https://doi.org/10.1039/c5cp06747b.

- 729 (37) Kamcev, J.; Paul, D. R.; Manning, G. S.; Freeman, B. D. Predicting Salt Permeability
- Coefficients in Highly Swollen, Highly Charged Ion Exchange Membranes. *Acs Appl Mater*
- 731 Inter 2017, 9 (4), 4044–4056. https://doi.org/10.1021/acsami.6b14902.
- 732 (38) Ju, H.; Sagle, A. C.; Freeman, B. D.; Mardel, J. I.; Hill, A. J. Characterization of Sodium
- 733 Chloride and Water Transport in Crosslinked Poly(Ethylene Oxide) Hydrogels. *J Membrane Sci*
- 734 **2010**, 358 (1–2), 131–141. https://doi.org/10.1016/j.memsci.2010.04.035.
- 735 (39) Calmon, C. Application of Volume Characteristics of Sulfonated Polystyrene Resins as a
- 736 Tool in Analytical Chemistry. *Anal Chem* **1953**, *25* (3), 490–492.
- 737 <u>https://doi.org/10.1021/ac60075a028</u>.
- 738 (40) Geise, G. M.; Hickner, M. A.; Logan, B. E. Ionic Resistance and Permselectivity Tradeoffs
- 739 in Anion Exchange Membranes. Acs Appl Mater Inter **2013**, 5 (20), 10294–10301.
- 740 <u>https://doi.org/10.1021/am403207w</u>.
- 741 (41) Sundheim, B. R.; Waxman, M. H.; Gregor, H. P. Studies on Ion Exchange Resins. VII.
- 742 Water Vapor Sorption by Cross-Linked Polystyrenesulfonic Acid Resins. J Phys Chem 1953, 57
- 743 (9), 974–978. https://doi.org/10.1021/j150510a029.
- 744 (42) Gregor, H. P.; Gutoff, F.; Bregman, J. I. Studies on Ion-Exchange Resins. II. Volumes of
- 745 Various Cation-Exchange Resin Particles. J Coll Sci Imp U Tok 1951, 6 (3), 245–270.
- 746 https://doi.org/10.1016/0095-8522(51)90043-8.
- 747 (43) Kamcev, J.; Paul, D. R.; Freeman, B. D. Effect of Fixed Charge Group Concentration on
- Equilibrium Ion Sorption in Ion Exchange Membranes. J Mater Chem A 2017, 5 (9), 4638–4650.
- 749 <u>https://doi.org/10.1039/c6ta079</u>54g.
- 750 (44) Kamcev, J.; Doherty, C. M.; Lopez, K. P.; Hill, A. J.; Paul, D. R.; Freeman, B. D. Effect of
- 751 Fixed Charge Group Concentration on Salt Permeability and Diffusion Coefficients in Ion
- 752 Exchange Membranes. *J Membrane Sci* **2018**, *566*, 307–316.
- 753 https://doi.org/10.1016/j.memsci.2018.08.053.
- 754 (45) Miller, D. J.; Houle, F. A. Integrated Solar Fuel Generators. *Energy Environ Ser* **2019**, 341–
- 755 385. https://doi.org/10.1039/9781788010313-00341.
- 756 (46) Yasuda, H.; Lamaze, C. E.; Peterlin, A. Diffusive and Hydraulic Permeabilities of Water in
- Water-swollen Polymer Membranes. J Polym Sci Part 2 Polym Phys 1971, 9 (6), 1117–1131.
- 758 https://doi.org/10.1002/pol.1971.160090608.
- 759 (47) Yasuda, H.; Lamaze, C. E.; Ikenberry, L. D. Permeability of Solutes through Hydrated
- 760 Polymer Membranes. Part I. Diffusion of Sodium Chloride. *Die Makromolekulare Chemie* **1968**,
- 761 *118* (1), 19–35. https://doi.org/10.1002/macp.1968.021180102.

- 762 (48) Payaka, A.; Tongraar, A.; Rode, B. M. QM/MM Dynamics of CH3COO—Water Hydrogen
- 763 Bonds in Aqueous Solution. *J Phys Chem* **2010**, *114* (38), 10443–10453.
- 764 https://doi.org/10.1021/jp105671f.
- 765 (49) Takano, M.; Ogata, K.; Kawauchi, S.; Satoh, M.; Komiyama, J. Ion-Specific Swelling
- 766 Behavior of Poly(N-Vinyl-2-Pyrrolidone) Gel: Correlations with Water Hydrogen Bond and
- Non-Freezable Water. *Polym Gels Netw* **1998**, *6* (3–4), 217–232. https://doi.org/10.1016/s0966-
- 768 7822(98)00015-x.
- 769 (50) Jang, E.-S.; Kamcev, J.; Kobayashi, K.; Yan, N.; Sujanani, R.; Dilenschneider, T. J.; Park,
- 770 H. B.; Paul, D. R.; Freeman, B. D. Influence of Water Content on Alkali Metal Chloride
- 771 Transport in Cross-Linked Poly(Ethylene Glycol) Diacrylate.1. Ion Sorption. *Polymer* **2019**, *178*,
- 772 121554. https://doi.org/10.1016/j.polymer.2019.121554.
- 773 (51) Kamcev, J.; Paul, D. R.; Manning, G. S.; Freeman, B. D. Accounting for Frame of
- Reference and Thermodynamic Non-Idealities When Calculating Salt Diffusion Coefficients in
- 775 Ion Exchange Membranes. *J Membrane Sci* **2017**, *537*, 396–406.
- 776 https://doi.org/10.1016/j.memsci.2017.05.034.
- 777 (52) Wu, Y.-H.; Park, H. B.; Kai, T.; Freeman, B. D.; Kalika, D. S. Water Uptake, Transport and
- 778 Structure Characterization in Poly(Ethylene Glycol) Diacrylate Hydrogels. *J Membrane Sci*
- **2010**, *347* (1–2), 197–208. https://doi.org/10.1016/j.memsci.2009.10.025.
- 780 (53) Geise, G. M.; Falcon, L. P.; Freeman, B. D.; Paul, D. R. Sodium Chloride Sorption in
- 781 Sulfonated Polymers for Membrane Applications. J. Membr. Sci. 2012, 423, 195–208.
- 782 https://doi.org/10.1016/j.memsci.2012.08.014.
- 783 (54) Yan, N.; Sujanani, R.; Kamcey, J.; Galizia, M.; Jang, E.-S.; Paul, D. R.; Freeman, B. D.
- 784 Influence of Fixed Charge Concentration and Water Uptake on Ion Sorption in AMPS/PEGDA
- 785 Membranes. J. Membr. Sci. **2022**, 644, 120171. https://doi.org/10.1016/j.memsci.2021.120171.
- 786 (55) Yu, Y.; Yan, N.; Freeman, B. D.; Chen, C.-C. Mobile Ion Partitioning in Ion Exchange
- 787 Membranes Immersed in Saline Solutions. J. Membr. Sci. 2021, 620, 118760.
- 788 https://doi.org/10.1016/j.memsci.2020.118760.
- 789 (56) Freger, V.; Bason, S. Characterization of Ion Transport in Thin Films Using
- 790 Electrochemical Impedance Spectroscopy I. Principles and Theory. J. Membr. Sci. 2007, 302 (1–
- 791 2), 1–9. https://doi.org/10.1016/j.memsci.2007.06.046.
- 792 (57) Bason, S.; Oren, Y.; Freger, V. Characterization of Ion Transport in Thin Films Using
- 793 Electrochemical Impedance Spectroscopy II: Examination of the Polyamide Layer of RO
- 794 Membranes. J. Membr. Sci. **2007**, 302 (1–2), 10–19.
- 795 https://doi.org/10.1016/j.memsci.2007.05.007.
- 796 (58) Wang, L.; Cao, T.; Pataroque, K. E.; Kaneda, M.; Biesheuvel, P. M.; Elimelech, M.
- 797 Significance of Co-Ion Partitioning in Salt Transport through Polyamide Reverse Osmosis

- Membranes. *Environ. Sci. Technol.* **2023**, *57* (9), 3930–3939. https://doi.org/10.1021/acs.est.2c09772.